Article

Morphological and Phylogenetic Evidence for Recognition of Two New Species of *Phanerochaete* from East Asia

Dong-Qiong Wang [1,2] and Chang-Lin Zhao [1,2,3,4,*]

1   Key Laboratory for Forest Resources Conservation and Utilization in the Southwest Mountains of China, Ministry of Education, Southwest Forestry University, Kunming 650224, China; fungiwangdongqiong@163.com
2   College of Biodiversity Conservation, Southwest Forestry University, Kunming 650224, China
3   Yunnan Key Laboratory for Fungal Diversity and Green Development, Kunming Institute of Botany, Chinese Academy of Sciences, Kunming 650201, China
4   School of Life Sciences, Tsinghua University, Beijing 100084, China
*   Correspondence: fungi@swfu.edu.cn or fungichanglinz@163.com

Abstract: Two new corticioid fungal species, *Phanerochaete pruinosa* and *P. rhizomorpha* spp. nov. are proposed based on a combination of morphological features and molecular evidence. *Phanerochaete pruinosa* is characterized by the resupinate basidiomata with the pruinose hymenial surface, a monomitic hyphal system with simple-septate generative hyphae and subcylindrical basidiospores measuring as 3.5–6.7 × 1.5–2.7 μm. *Phanerochaete rhizomorpha* is characterized by having a smooth hymenophore covered by orange hymenial surface, the presence of rhizomorphs, subulate cystidia, and narrower ellipsoid to ellipsoid basidiospores. Sequences of ITS+nLSU nrRNA gene regions of the studied specimens were generated and phylogenetic analyses were performed with maximum likelihood, maximum parsimony, and Bayesian inference methods. These phylogenetic analyses showed that two new species clustered into genus *Phanerochaete*, in which *P. pruinosa* was sister to *P. yunnanensis* with high supports (100% BS, 100% BT, 1.00 BPP); morphologically differing by a pale orange to greyish orange and densely cracked hymenial surface. Another species *P. rhizomorpha* was closely grouped with *P. citrinosanguinea* with lower supports; morphologically having yellow to reddish yellow hymenial surface, and smaller cystidia measuring as 31–48 × 2.3–4.8 μm.

Keywords: corticioid fungi; Phanerochaetaceae; molecular systematics; taxonomy; Yunnan Province

1. Introduction

Corticioid fungi is a large group of Basidiomycota with simpler basidiomata with the diverse morphological features when compared with polypores, but the phylogenetic diversity of this group is less intensively studied [1,2]. In the subtropical–tropical areas, many corticioid taxa have not been discovered and described worldwide. The genus *Phanerochaete* P. Karst. is a member of the corticioid fungi, which is typified by *P. alnea* (Fr.) P. Karst. [3], and the genus is characterized by the resupinate, membranaceous basidiomata with or without rhizomorphs, a monomitic hyphal system with primarily simple-septate generative hyphae, clavate basidia with four sterigmata, and smooth, thin-walled, inamyloid basidiospores [1,4,5]. Index Fungorum (http://www.indexfungorum.org; accessed on 9 December 2021) registers 187 specific and infraspecific names in *Phanerochaete*. The diversity and taxonomy of *Phanerochaete* s.l. in China have been studied for the last 30 years [6–19].

Molecular studies involving *Phanerochaete* based on the ribosomal DNA (rDNA) sequences, revealed the phylogenetic distribution of resupinate forms across the major clades of mushroom-forming fungi, in which *P. chrysosporium* Burds. nested into phlebioid clade in Polyporales [20]. Revisiting the taxonomy of *Phanerochaete* (Polyporales, Basidiomycota) using a four gene dataset and extensive ITS sampling indicated that *Phanerochaete* sensu lato was polyphyletic and distributed across nine lineages in the phlebioid clade, in which

six lineages were associated to described genera [21]. Miettinen et al. [22]. explored the DNA-phylogeny-based and morphology-based to reconcile the polypores and genus concepts in the family Phanerochaetaceae, which the macromorphology of fruiting bodies and hymenophore construction did not reflect monophyletic groups, and *Ceriporia inflata* B.S. Jia and B.K. Cui was combined into *Phanerochaete*. Amplifying nrLSU, nrITS, and rpb1 genes across the Polyporales revealed that eleven genera clustered into family Phanerochaetaceae, and two families Hapalopilaceae and Bjerkanderaceae were placed as synonyms of Phanerochaetaceae [23]. Recently, the research supported by morphological studies and the phylogenetic analyses, showed that many new taxa of *Phanerochaete* s.s. were found and displayed the taxonomic status for the new taxa within genus *Phanerochaete* [14,19].

In 2018–2019, we collected the material supposedly belonging to the two undescribed species of corticioid fungi from Yunnan Province, China. We present the morphological and molecular phylogenetic evidence that support the recognition of two new species within the *Phanerochaete* s.s., based on the internal transcribed spacer (ITS) and regions nLSU sequences.

2. Materials and Methods

2.1. Morphology

The fruiting bodies were observed growing on the ground of broad-leaved treemixed forest. The fruiting bodies were dried in an electric food dehydrator at 40 °C, then sealed and stored in an envelope bag. They were then transported to Kunming where microscopic morphology and phylogeny to be studied at the mycology laboratory of Southwest Forestry University, Kunming, Yunnan Province, China. The for-study specimens were deposited at the herbarium of Southwest Forestry University (SWFC), Kunming, Yunnan Province, China. Macromorphological descriptions were based on field notes and photos captured in the field and lab. Color terminology follow Petersen [24]. Micromorphological data were obtained from the dried specimens, and observed under a light microscope following Dai [25]. The following abbreviations were used: KOH = 5% potassium hydroxide water solution, CB = Cotton Blue, CB– = acyanophilous, IKI = Melzer's reagent, IKI– = both inamyloid and indextrinoid, L = mean spore length (arithmetic average for all spores), W = mean spore width (arithmetic average for all spores), Q = variation in the L/W ratios between the specimens studied, $n = a/b$ (number of spores (a) measured from given number of specimens (b)).

2.2. Molecular Phylogeny

CTAB rapid plant genome extraction kit-DN14 (Aidlab Biotechnologies Co., Ltd., Beijing, China) was used to obtain genomic DNA from dried specimens, according to the manufacturer's instructions followed previous study [26]. ITS region was amplified with primer pair ITS5 and ITS4 [27]. nLSU region was amplified with primer pair LR0R and LR7 (http://lutzonilab.org/nuclear-ribosomal-dna/; accessed on 28 September 2021). The PCR procedure for ITS was as follows: initial denaturation at 95 °C for 3 min, followed by 35 cycles at 94 °C for 40 s, 58 °C for 45 s, and 72 °C for 1 min, and a final extension of 72 °C for 10 min. The PCR procedure for nLSU was as follows: initial denaturation at 94 °C for 1 min, followed by 35 cycles at 94 °C for 30 s, 48 °C for 1 min and 72 °C for 1.5 min, and a final extension of 72 °C for 10 min. The PCR products were purified and directly sequenced at Kunming Tsingke Biological Technology Limited Company, Kunming, Yunnan Province, China. All newly generated sequences were deposited in NCBI GenBank (Table 1).

Table 1. List of species, specimens, and GenBank accession numbers of sequences used in this study.

Species Name	Specimen No.	GenBank Accession No.		References
		ITS	nLSU	
Bjerkandera adusta	FP-101236	KP134982		[21]
B. adusta	HHB-12826	KP134983	KP135198	[21]
B. fumosa	Dai 12674B	MW507112	MW520213	[28]

Table 1. *Cont.*

Species Name	Specimen No.	GenBank Accession No.		References
		ITS	nLSU	
B. fumosa	Dai 21087	MW507110		[28]
Byssomerulius corium	FP-102382	KP135007	KP135230	[21]
B. corium	FP-107055	KP135008		[21]
Ceraceomyces serpens	HHB-15692-Sp	KP135031	KP135200	[21]
C. serpens	L-11105	KP135032		[21]
Ceriporia purpurea	KKN-223-Sp	KP135044	KP135203	[21]
C. purpurea	HHB-3964	KP135042		[21]
C. reticulata	RLG-11354	KP135041	KP135204	[21]
C. reticulata	L-7837	KP135040		[21]
Efibula gracilis	FD-455	KP135027	MZ637116	[21]
E. gracilis	FP-102052	KP135028		[21]
E. tropica	Wu 0809-8	MZ636968	MZ637130	unpublished
E. tropica	WEI 18-149	MZ636967	MZ637129	unpublished
Gloeoporus dichrous	FP-151129	KP135058	KP135213	[21]
G. pannocinctus	L-15726-Sp	KP135060	KP135214	[21]
Hyphodermella poroides	Dai 12045	KX008367	KX011852	[29]
H. poroides	Dai 10848	KX008368	KX011853	[29]
H. rosae	FP-150552	KP134978	KP135223	[21]
H. rosae	MA-Fungi	FN600389	JN939588	[30]
Irpex lacteus	FD-9	KP135026	KP135224	[21]
I. lacteus	FD-93	KP135025		[21]
Meruliopsis albostramineus	HHB-10729	KP135051	KP135229	[21]
M. albostramineus	L-9778	KP135052		[21]
M. taxicola	CBS 45548	MH856432	MH867978	[31]
M. taxicola	Kuljok 00/75 (GB)	EU118648		[32]
Phaeophlebiopsis caribbeana	HHB-6990	KP135415	KP135243	[21]
P. caribbeana	FD-442 (TYPE)	KP135416		[21]
P. ignerii	FD-425	KP135418		[21]
P. peiophoroides	FP-150577	KP135417	KP135273	[21]
Phanerochaete. albida	FD-31	KP135308	KP135210	[19]
P. alnea	OM 8110	KP135171		[21]
P. alnea	KHL 12054	EU118653	EU118653	[32]
P. argillacea	Wu 9712-18		GQ470656	[13]
P. arizonica	RLG-10248-sp	KP135170	KP135239	[21]
P. australis	He 6013	MT235656	MT248136	[19]
P. australis	HHB-7105-sp	KP135081	KP135240	[21]
P. australosanguinea	20098 Tell		MH233928	[33]
P. australosanguinea	20102 Tell		MH233929	[33]
P. bambucicola	He 3606	MT235657	MT248137	[19]
P. bambucicola	Wu 0707-2	MF399404	MF399395	[15]
P. brunnea	He 4192	MT235658	MT248138	[19]
P. brunnea	He 1873	KX212220	KX212224	[17]
P. burdsallii	He 2066	MT235690	MT248177	[19]
P. burdsallii	CFMR: RF9JR	KU668973		unpublished
P. burtii	HHB-4618-sp	KP135117	KP135241	[21]
P. burtii	FD-171	KP135116		[21]
P. calotricha	Vanhanen-382	KP135107		[21]
P. canobrunnea	He 5726	MT235659	MT248139	[19]
P. canobrunnea	CHWC 1506-66	LC412095	LC412104	[14]
P. canolutea	Wu 9211-105		GQ470641	[13]
P. carnosa	He 5172	MT235660	MT248140	[19]
P. carnosa	HHB-9195	KP135129	KP135242	[21]
P. chrysosporium	HHB-6251	KP135094	KP135246	[21]
P. chrysosporium	He 5778	MT235661	MT248141	[19]

Table 1. *Cont.*

Species Name	Specimen No.	GenBank Accession No.		References
		ITS	**nLSU**	
P. cinerea	He 6003		MT248172	[19]
P. citrinosanguinea	He 4298	MT235691	MT248178	[19]
P. citrinosanguinea	FP-105385-sp	KP135100	KP135234	[21]
P. concrescens	He 4657	MT235662	MT248142	[19]
P. concrescens	Spirin 7322	KP994380	KP994382	[34]
P. cumulodentata	He 2995	MT235664	MT248144	[19]
P. cumulodentata	LE 298935	KP994359	KP994386	[34]
P. cystidiata	He 4224	MT235665	MT248145	[19]
P. cystidiata	Wu 1708-326	LC412097	LC412100	[14]
P. deflectens	FCUG 2777		GQ470644	[13]
P. ericina	He 4285	MT235666	MT248146	[19]
P. ericina	HHB-2288	KP135167	KP135247	[21]
P. exilis	HHB-6988	KP135001	KP135236	[21]
P. fusca	Wu 1409-163	LC412099	LC412106	[14]
P. hymenochaetoides	He 5988		MT248173	[19]
P. incarnata	He 20120728-1	MT235669	MT248149	[19]
P. incarnata	WEI 16-075	MF399406	MF399397	[15]
P. inflata	Dai 10376	JX623929	JX644062	[35]
P. inflata	Cui 7712	JX623930	JX644063	[35]
P. krikophora	HHB-5796	KP135164	KP135268	[21]
P. laevis	He 20120917-8	MT235670	MT248150	[19]
P. laevis	HHB-15519	KP135149	KP135249	[21]
P. leptocystidiata	He 5853	MT235685	MT248168	[19]
P. leptocystidiata	Dai 10468	MT235684	MT248167	[19]
P. livescens	He 5010	MT235671	MT248151	[19]
P. livescens	FD-106	KP135070	KP135253	[21]
P. magnoliae	He 3321	MT235672	MT248152	[19]
P. magnoliae	HHB-9829-sp	KP135089	KP135237	[21]
P. metuloidea	He 2565		MT248163	[19]
P. metuloidea	He 2766	MT235682	MT248164	[19]
P. minor	He 3988	MT235686	MT248170	[19]
P. minor	He 3977		MT248169	[19]
P. parmastoi	He 4570	MT235673	MT248153	[19]
P. parmastoi	Wu 880313-6		GQ470654	[13]
P. porostereoides	He 1902	KX212217	KX212221	[17]
P. pruinosa	**CLZhao 7712**	**MZ435346**	**MZ435350**	**Present study**
P. pruinosa	**CLZhao 7713**	**MZ435347**	**MZ435351**	**Present study**
P. pseudomagnoliae	PP-25	KP135091	KP135250	[21]
P. pseudosanguinea	FD-244	KP135098	KP135251	[21]
P. queletii	HHB-11463	KP134994	KP135235	[21]
P. queletii	FP-102166	KP134995		[21]
P. rhizomorpha	**CLZhao 10470**	**MZ435348**	**MZ435352**	**Present study**
P. rhizomorpha	**CLZhao 10477**	**MZ435349**	**MZ435353**	**Present study**
P. rhodella	FD-18	KP135187	KP135258	[21]
P. robusta	Wu 1109-69	MF399409	MF399400	[15]
P. robusta	Ghobad 2288	KP127068	KP127069	[16]
P. sanguinea	HHB-7524	KP135101	KP135244	[21]
P. sanguineocarnosa	FD-359	KP135122	KP135245	[21]
P. sinensis	He 4660	MT235688	MT248175	[19]
P. sinensis	GC 1809-56	MT235689	MT248176	[19]
P. sordida	He 5400	MT235676	MT248157	[19]
P. sordida	FD-241	KP135136	KP135252	[21]
P. stereoides	He 5824	MT235677	MT248158	[19]
P. subceracea	FP-105974-R	KP135162	KP135255	[21]
P. subrosea	He 2421	MT235687	MT248174	[19]
P. taiwaniana	He 5269	MT235680	MT248161	[19]

Table 1. *Cont.*

| Species Name | Specimen No. | GenBank Accession No. | | References |
		ITS	nLSU	
P. taiwaniana	Wu 0112-13	MF399412	MF399403	[15]
P. thailandica	2015_07	MF467737		[36]
P. velutina	He 3079	MT235681	MT248162	[19]
P. velutina	Kotiranta 25567	KP994354	KP994387	[34]
P. xerophila	HHB-8509-Sp	KP134996	KP135259	[21]
P. xerophila	KKN-172	KP134997		[21]
P. yunnanensis	He 2719	MT235683	MT248166	[19]
P. yunnanensis	He 2697		MT248165	[19]
Phlebiopsis flavidoalba	FD-263	KP135402	KP135271	[21]
P. flavidoalba	FD-374	KP135403		[21]
P. gigantea	FP-70857-sp	KP135390	KP135272	[21]
P. gigantea	FP-101815	KP135389		[21]
Pirex concentricus	OSC-41587	KP134984	KP135275	[21]
P. concentricus	Kropp160Bup6-R	KP134985		[21]
Rhizochaete filamentosa	HHB-3169	KP135410	KP135278	[21]
R. filamentosa	FP-105240	KP135411		[21]
R. radicata	FD-123	KP135407	KP135279	[21]
Terana caerulea	FP-104073	KP134980	KP135276	[21]
T. caerulea	T-616	KP134981		[21]
Trametopsis aborigena	Robledo 1238	KY655337		[37]
T. aborigena	Robledo 1236	KY655336		[37]
T. cervina	AJ-185	JN165020	JN164839	[21]
T. cervina	AJ-189	JN165021		[21]

New sequences are shown in bold.

Sequences were aligned in MAFFT 7 (https://mafft.cbrc.jp/alignment/server/; accessed on 28 September 2021) using G-INS-i strategy for ITS+nLSU combined dataset, and manually adjusted in BioEdit [38]. Aligned dataset was deposited in TreeBase (submission ID 28442). *Phlebiopsis gigantea* Fr. and *Rhizochaete radicata* (Henn.) Gresl., Nakasone and Rajchenb were selected as an outgroup for phylogenetic analyses of combined dataset following a previous study [19]. The taxon sampling strategy for the selection of sequences for phylogenetic trees was to choose (1) in a larger scale, focusing on the related genera in the families Phanerochaetaceae and Irpicaceae in Figure 1; (2) the related taxa based on BLAST search in GenBank within *Phanerochaete* s.l.; and (3) all species of *Phanerochaete* s.s.

Maximum parsimony analysis was applied to the combined (ITS+nLSU) dataset. Its approaches followed Zhao and Wu [26], and the tree construction procedure was performed in PAUP* version 4.0b10 [39]. All characters were equally weighted and gaps were treated as missing data. Trees were inferred using the heuristic search option with TBR branch swapping and 1000 random sequence additions. Max-trees were set to 5000, branches of zero length were collapsed and all parsimonious trees were saved. Clade robustness was assessed using bootstrap (BT) analysis with 1000 replicates [40]. Descriptive tree statistics: tree length (TL), consistency index (CI), retention index (RI), rescaled consistency index (RC), and homoplasy index (HI) were calculated for each Maximum Parsimonious Tree generated. Datamatrix was also analyzed using Maximum Likelihood (ML) approach with RAxML-HPC2 through the CIPRES Science Gateway (www.phylo.org; accessed on 28 September 2021) [41]. Branch support (BS) for ML analysis was determined by 1000 bootstrap replicates.

MrModeltest 2.3 [42] was used to determine the best-fit evolution model for the dataset for Bayesian inference (BI). BI was calculated with MrBayes 3.1.7a [43]. Four Markov chains were run for 2 runs from random starting trees for 10 million generations for ITS+nLSU (Figure 2). The first one-fourth of all generations was discarded as burn-in. The majority rule consensus tree of all remaining trees was calculated. Branches were considered as significantly supported if they received maximum likelihood bootstrap

value (BS) >70%, maximum parsimony bootstrap value (BT) >70%, or Bayesian posterior probabilities (BPP) >0.95.
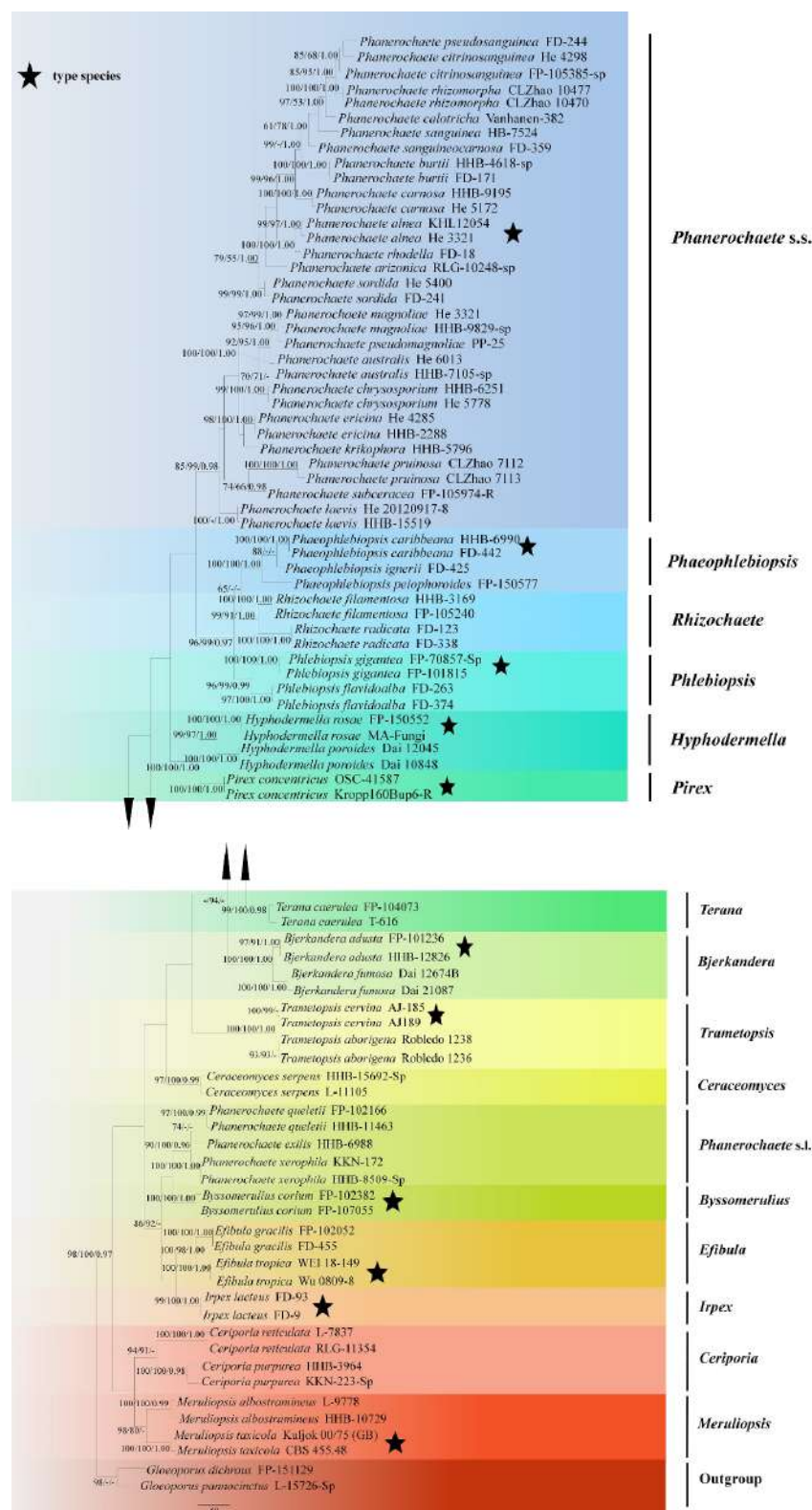
Figure 1. Maximum Parsimony strict consensus tree illustrating the phylogeny of two new species and related genera in Phanerochaetaceae and Irpicaceae based on ITS+nLSU sequences. Branches are labeled with maximum likelihood bootstrap values >70%, parsimony bootstrap values >70% and Bayesian posterior probabilities >0.95, respectively.
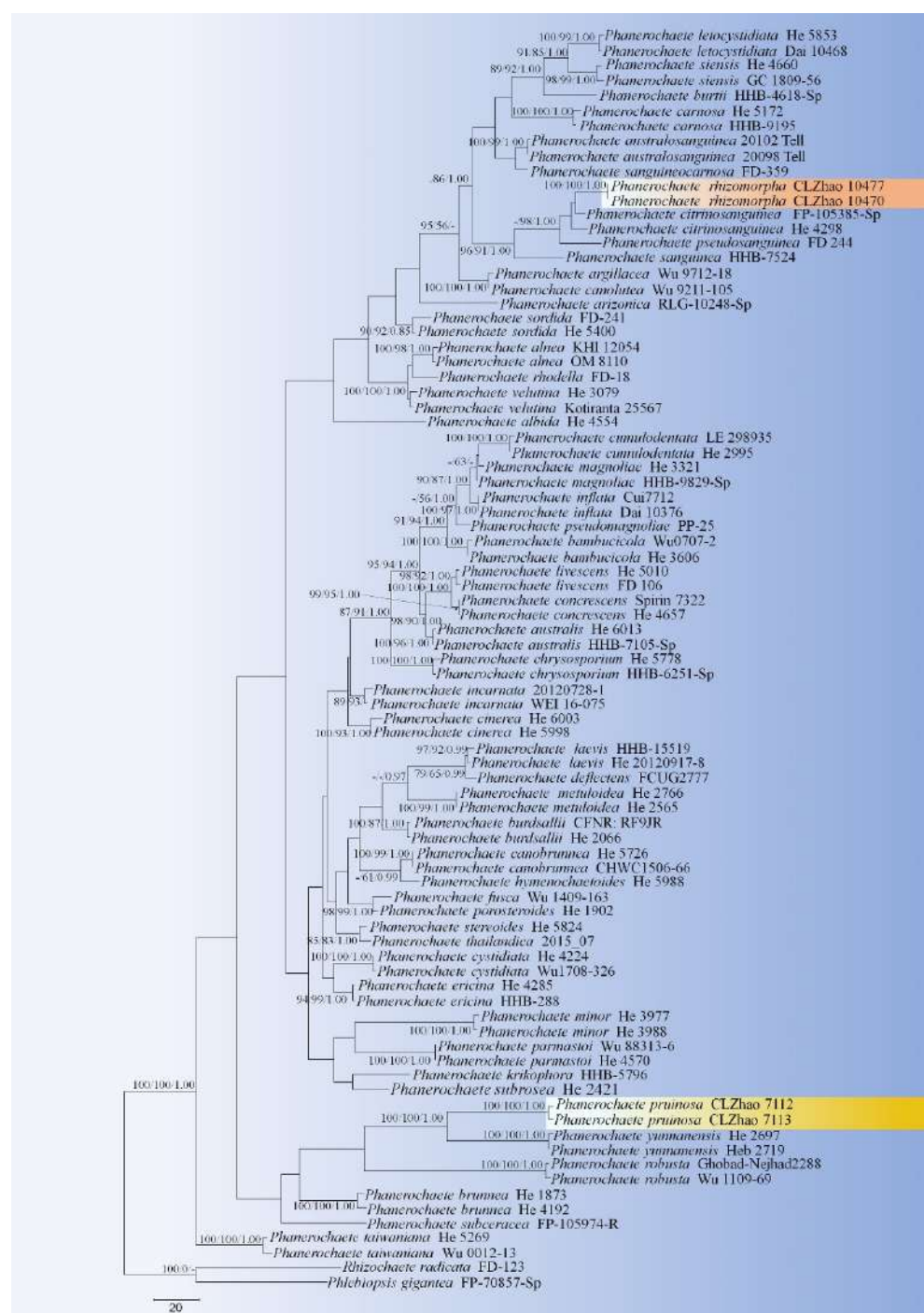
Figure 2. Maximum Parsimony strict consensus tree illustrating the phylogeny of two new species and related species in *Phanerochaete* based on ITS+nLSU sequences. Branches are labeled with maximum likelihood bootstrap values >70%, parsimony bootstrap values >70% and Bayesian posterior probabilities >0.95, respectively. The yellow backgrounds indicate new species.

3. Results

3.1. Molecular Phylogeny

The ITS+nLSU dataset (Figure 1) included sequences from 86 fungal specimens representing 50 species. The dataset had an aligned length of 2368 characters, of which 1170 characters are constant, 598 are variable and parsimony-uninformative, and 600 are parsimony-informative. Maximum parsimony analysis yielded one equally parsimonious tree (TL = 3476, CI = 0.3631, HI = 0.6369, RI = 0.7539, RC = 0.3512). Best model for the

ITS+nLSU dataset estimated and applied in the Bayesian analysis was GTR+I+G (lset nst = 6, rates = invgamma; prset statefreqpr = dirichlet (1,1,1,1)). Bayesian analysis and ML analysis resulted in a similar topology to MP analysis with an average standard deviation of split frequencies = 0.038487 (BI), and the effective sample size (ESS) across the two runs is the double of the average ESS (avg ESS) = 303.

The phylogeny (Figure 1) based on the combined ITS+nLSU sequences indicated that both species *Phanerochaete pruinose* and *P. rhizomorpha* clustered into *Phanerochaete* s.s and then *P. pruinose* grouped with *P. subceracea* (Burt) Burds.; *P. rhizomorpha* was sister to *P. citrinosanguinea* Floudas and Hibbett.

The ITS+nLSU dataset (Figure 2) included sequences from 83 fungal specimens representing 53 taxa. The dataset had an aligned length of 2017 characters, of which 1548 characters are constant, 164 are variable and parsimony-uninformative, and 395 are parsimony-informative. Maximum parsimony analysis yielded 35 equally parsimonious trees (TL = 1900, CI = 0.4095, HI = 0.5905, RI = 0.6456, RC = 0.2644). Best model for the ITS+nLSU dataset estimated and applied in the Bayesian analysis was GTR+I+G (lset nst = 6, rates = invgamma; prset statefreqpr = dirichlet (1,1,1,1)). Bayesian analysis and ML analysis resulted in a similar topology to MP analysis with an average standard deviation of split frequencies = 0.004260 (BI), and the effective sample size (ESS) across the two runs is the double of the average ESS (avg ESS) = 309.

The phylogram inferred from ITS+nLSU sequences (Figure 2) revealed that two new species were clustered into genus *Phanerochaete* s.s.; *P. pruinosa* sp. nova. was sister to *P. yunnanensis* Y.L. Xu and S.H. He with high supports (100% BS, 100% BT, 1.00 BPP), and then grouped with *P. robusta* Parmasto without supported data. Another species *P. rhizomorpha* sp. nova. was closely grouped with *P. citrinosanguinea* with lower supports, and then grouped with *P. pseudosanguinea* Floudas and Hibbett (–BS, 98% BP and 1.00 BPP) and *P. sanguinea* (Fr.) Pouzar (96% BS, 91% BP and 1.00 BPP).

3.2. Taxonomy

Phanerochaete pruinosa C.L. Zhao and D.Q. Wang, sp. nov. Figures 3 and 4.
MycoBank no.: MB 841271.
Diagnosis: It differs from *P. yunnanensis* by its pruinose hymenophore with the white to slightly cream hymenial surface and lightly darkening in KOH.

Holotype—China, Yunnan Province, Chuxiong, Zixishan National Forestry Park, on the bark of fallen angiosperms, 101.4° E, 25.1° N, 1 July 2018, CLZhao 7113 (SWFC).

Etymology—*pruinosa* (Lat.): from Latin, referring to the white powder on hymenial surface of basidiomata.

Fruiting body—Basidiomata annual, resupinate, adnate, undetachable from substrate, membranaceous to coriaceous, without odor and taste when fresh, up to 15 cm long, 3 cm wide, 50–100 μm thick. Hymenial surface smooth to have small verrucous process, pruinose, white when fresh, white to slightly cream on drying; lightly darkening in KOH. Margin sterile, narrow, white, attached.

Hyphal system—Hyphal system monomitic, generative hyphae simple-septa, colorless, thick-walled, unbranched, interwoven, 3–4.5 μm in diameter, subhymenial hyphae densely covered by larger crystals, basal hyphae regular; IKI–, CB–; tissues unchanged in KOH.

Hymenium—Hymenial cystidia and cystidoles absent; basidia clavate to subcylindrical, with four sterigmata and a simple-septum, 13–24 μm × 3.5–4.5 μm.

Spores—Basidiospores cylindrical, colorless, thin-walled, smooth, IKI–, CB–, (3.3–)3.5–6.7(–7) μm × 1.5–2.7(–2.9) μm, L = 4.42 μm, W = 1.94 μm, Q = 2.21–2.35 (n = 60/2).

Additional specimen examined—China, Yunnan Province, Zixishan National Forestry Park, on fallen branch of angiosperm, 101.4° E, 25.1° N, 1 July 2018, C.L. Zhao 7112 (SWFC).

Habitat and ecology—Climate of the sample collection site is monsoon humid, and the forest type is evergreen broad-leaved forest, and the samples were collected on an angiosperm branch.
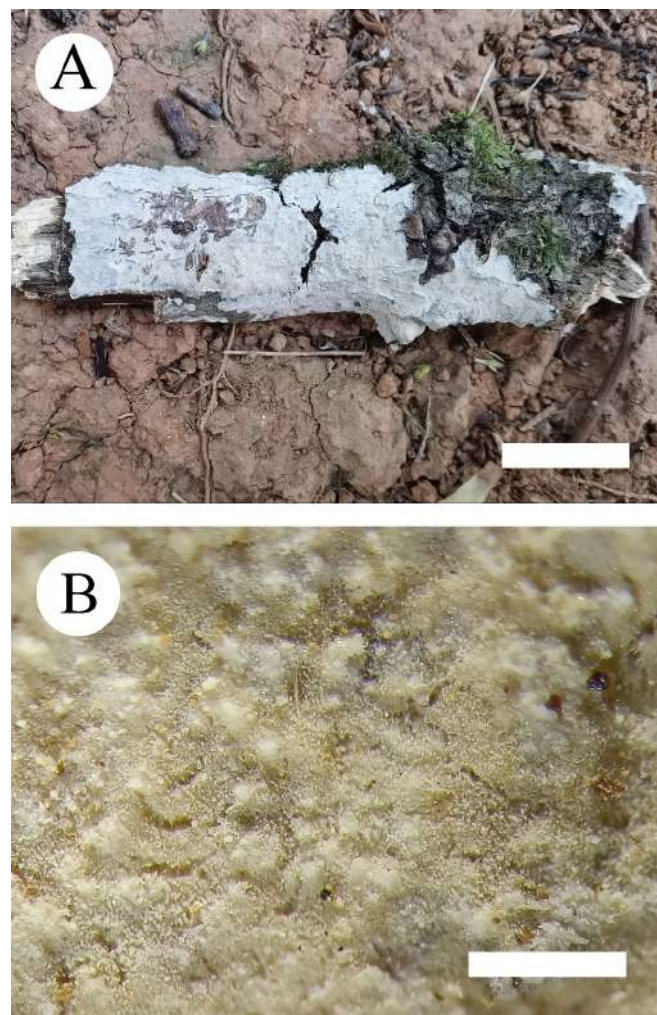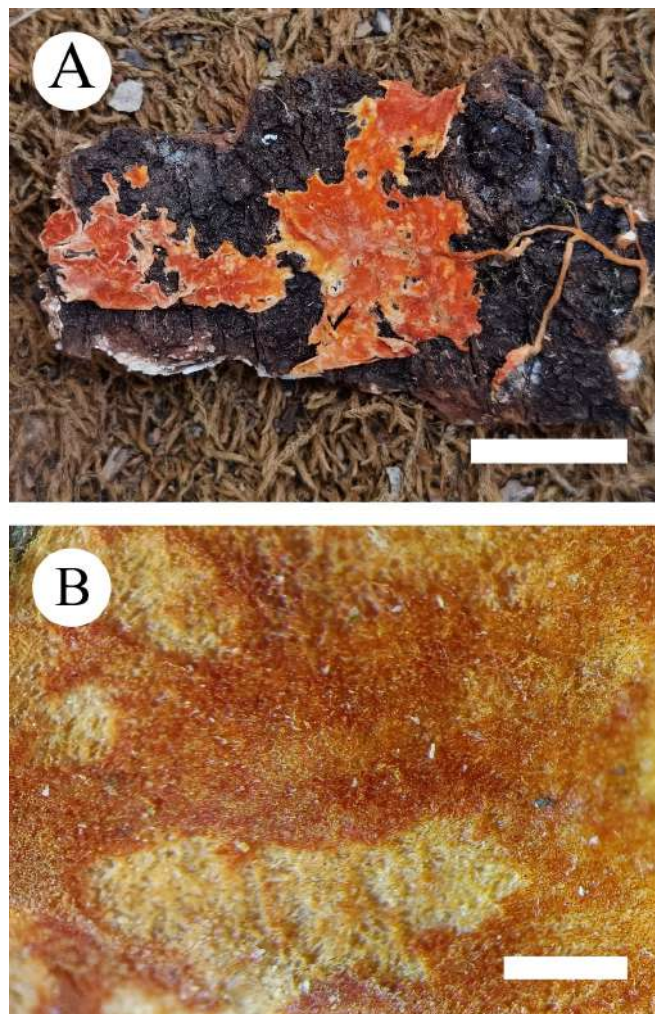
**Figure 3.** Basidiomata of *Phanerochaete pruinosa* (holotype) Bars: (**A**) = 2 cm and (**B**) = 1 mm.
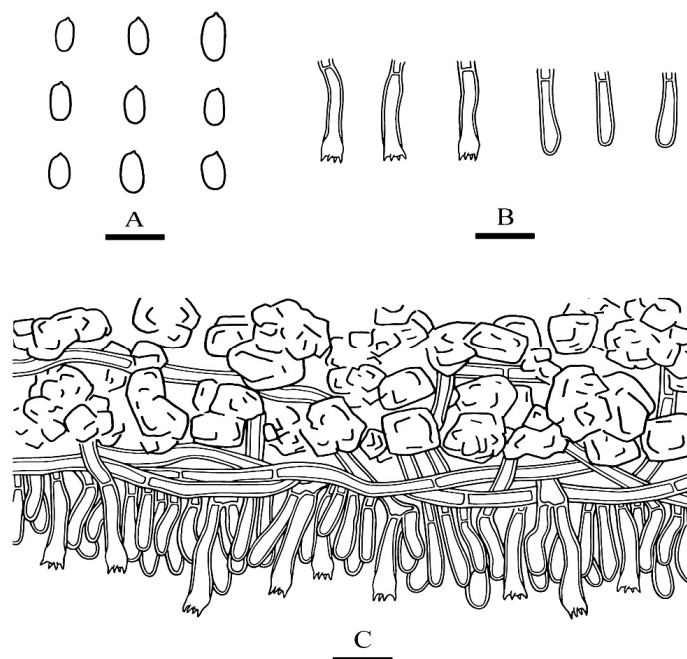
Figure 4. Microscopic structures of *Phanerochaete pruinosa* (holotype): basidiospores (**A**), basidia and basidioles (**B**), A section of hymenium (**C**). Bars: (**A**) = 5 μm, (**B**,**C**) = 10 μm.

Phanerochaete rhizomorpha C.L. Zhao and D.Q. Wang sp. nov. Figures 5 and 6.

Figure 5. Basidiomata of *Phanerochaete rhizomorpha* (holotype) Bars: (**A**) = 2 cm and (**B**) = 1 mm.
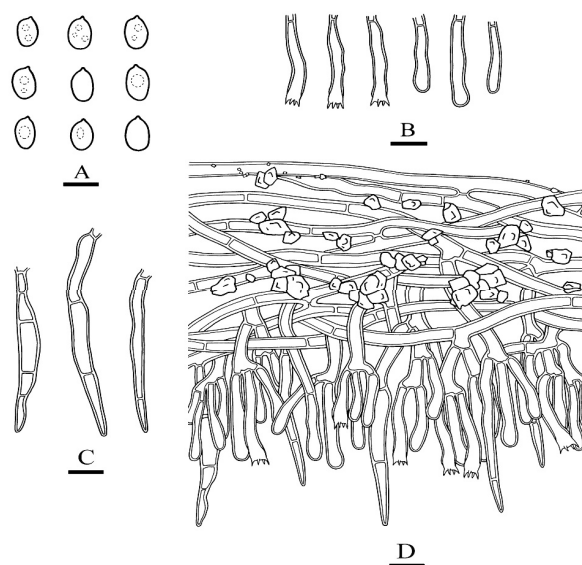
Figure 6. Microscopic structures of *Phanerochaete rhizomorpha* (holotype): basidiospores (**A**), basidia and basidioles (**B**), cystidia (**C**). A section of hymenium (**D**). Bars: (**A**) = 5 μm, (**B**–**D**) = 10 μm.

MycoBank no.: MB 841272.

Diagnosis: It differs from *P. citrinosanguinea* by its orange hymenial surface and larger cystidia 48.5–71.5 μm × 3–6.5 μm)

Holotype—China, Yunnan Province, Dali, Nanjian Country, Lingbaoshan National Forestry Park, on the fallen branch of angiosperm, 24.7° N, 100.6° E, 10 January 2019, C.L. Zhao 10,477 (SWFC).

Etymology—*rhizomorpha* (Lat.): from Latin, referring to the rhizomorphic basidiomata of the specimens.

Fruiting body—Basidiomata annual, resupinate, adnate, easily detachable from substrate, membranaceous, up to 5 cm long, 3 cm wide, 200–300 μm thick. Hymenial surface smooth, slightly orange when fresh, orange upon drying; lightly darkening in KOH. Margin sterile, buff to slightly orange, up to 1 mm wide, rhizomorphic.

Hyphal system—Hyphal system monomitic, generative hyphae simple-septa, colorless, thick-walled, frequently branched, interwoven, 3–6.5 μm in diameter, basal hyphae regular, numerous crystals present among the abhymenium hyphae, IKI–, CB–; tissues unchanged in KOH.

Hymenium—Hymenium cystidia subulate or tapering, colorless, thick-walled, with 2–4 septa, 48.5–71.5 μm × 3–6.5 μm; basidia subcylindrical, with 4 sterigmata, 18.5–35.5 μm × 3.5–5.5 μm.

Spores—Basidiospores narrower ellipsoid to ellipsoid, colorless, thin-walled, smooth, with oil 1–2 drops inside, IKI–, CB–, 4.5–5.8(–6) μm × 2.7–3.6(–3.8) μm, L = 5.07 μm, W = 3.19 μm, Q = 1.58–1.60 (n = 62/2).

Additional specimen examined—China, Yunnan Province, Nanjian Country, Lingbaoshan National Forestry Park, on fallen branch of angiosperm, 24.7° N, 100.6° E, 10 January 2019, C.L. Zhao 10,470 (SWFC).

Habitat and ecology—Climate of the sample collection site is a transition between tropical and subtropical climate, and the forest type is the tropical monsoon evergreen broad-leaved forest, and the samples were collected on an angiosperm trunk.

4. Discussion

In the present study, two new species, *Phanerochaete pruinosa* C.L. Zhao and D.Q. Wang and *P. rhizomorpha* C.L. Zhao and D.Q. Wang spp. nov., are described based on phylogenetic analyses and morphological characters. The nucleotide differences of phylogenetically similar species to *Phanerochaete pruinosa* and *P. rhizomorpha*.

Phylogenetically, Xu et al. [19] revealed the taxonomy and phylogeny of *Phanerochaete sensu stricto* (Polyporales, Basidiomycota) with emphasis on Chinese collections, which showed that twenty-eight species of *Phanerochaete* s.s. from China are confirmed by morphology and DNA sequence data. In the present study (Figure 2), two new taxa clustered into *Phanerochaete* s.s., in which *P. pruinosa* was sister to *P. yunnanensis*, and then grouped with *P. robusta*. Another species *P. rhizomorpha* was closely grouped with *P. citrinosanguinea* with lower supports, and then grouped with *P. pseudosanguinea* and *P. sanguinea*. However, morphologically, *P. yunnanensis* is separated from *P. pruinosa* by having a pale orange to greyish orange and densely cracked hymenial surface [19]; *P. robusta* differs in its yellow basidiomata and two kinds of cystidia without encrustation, larger basidiospores (5.5–7 μm × 2.4–2.9 μm) and a boreal distribution [34]. *Phanerochaete citrinosanguinea* differs from *P. rhizomorpha* by having yellow to reddish yellow hymenial surface, and smaller cystidia (31–48 μm × 2.3–4.8 μm) [21]; *P. pseudosanguinea* differs *P. rhizomorpha* in its light red or dark red hymenial surface, and narrower basidiospores (4–5.5 μm × 2–2.5 μm) [21]; *P. sanguinea* is separated from *P. rhizomorpha* by having the thin-walled cystidia and the larger basidia (25–45 μm × 4–6 μm) [1]; in addition, there is some coloration of wood as in *P. sanguinea*.

Morphologically, *Phanerochaete pruinosa* is similar to *P. concrescens* Spirin and Volobuev and *P. sordida* (P. Karst.) J. Erikss. and Ryvarden, based on presence of white or cream hymenial surface. However, *P. concrescens* differs from *P. pruinosa* by having the large

basidia (27–39 μm × 4–5 μm) [34]; *P. sordida* is separated from *P. pruinosa* by presence of cystidia and wider basidiospores (5–7 μm × 2.5–3.5 μm) [1].

Phanerochaete rhizomorpha reminds four taxa of *Phanerochaete* based on the character by having the rhizomorph, *P. burdsallii* Y.L. Xu, Nakasone and S.H. He, *P. leptocystidiata* Y.L. Xu and S.H. He, *P. sinensis* Y.L. Xu, C.C. Chen and S.H. He and *P. subrosea* Y.L. Xu and S.H. He. However, *P. burdsallii* differs from *P. rhizomorpha* by having the cystidia encrusted with small crystals [19]; *P. leptocystidiata* differs in having a tuberculate hymenial surface and thin-walled cystidia encrusted at apex (24–30 μm × 4–6 μm) [19]; *P. sinensis* differs in its thin-walled cystidia and the shorter basidia (17–22 μm × 4–5 μm) [19]; *P. subrosea* is separated from *P. rhizomorpha* by having the thin-walled and smaller cystidia (33–55 μm × 3–5 μm) [19].

Phanerochaete rhizomorpha is similar to *P. aurantiobadia* Ghob.-Nejh., S.L. Liu, Langer and Y.C. Dai, *P. cumulodentata* (Nikol.) Parmasto and *P. hymenochaetoides* Y.L. Xu and S.H. He based on the character by the orange hymenial surface. However, *P. aurantiobadia* differs from *P. rhizomorpha* by having the larger basidiospores (5–8.3 μm × 2–3 μm) [16]; *P. cumulodentata* differs from *P. rhizomorpha* by a tuberculate hymenophore and shorter basidia (16.7–28.3 μm × 3.7–5.2 μm) [34]; *P. hymenochaetoides* differs from *P. rhizomorpha* by having both smaller cystidia (30–45 μm × 3–4 μm) and basidiospores (4–5.2 μm × 2–2.8 μm) [19].

In the ecology and biogeography, the taxa of *Phanerochaete* are a typical example of wood-rotting fungi, which are mainly distributed in Asia, Europe, and America, and the substrata are mostly hardwood [1,25], and this genus is an extensively studied group of Basidiomycota; nonetheless, the wood-rotting fungi diversity is still not well known in the subtropics and tropics [44–48]. The two new species, *Phanerochaete pruinosa* and *P. rhizomorpha* spp. nov., were found in subtropics, which enriches the diversity of wood-rotting fungi.

References

1. Bernicchia, A.; Gorjón, S.P. *Fungi Europaei 12: Corticiaceae s.l. Edizioni Candusso, Lomazzo*; Candusso Edizioni: Origgio, Italy, 2010.
2. Larsson, K.-H.; Larsson, E.; Kõljalg, U. High phylogenetic diversity among corticioid homobasidiomycetes. *Mycol. Res.* **2004**, *108*, 983–1002. [CrossRef]
3. Karsten, P. Kritisk öfversigt af Finlan's Basidsvamper (Basidiomycetes, Gaster and Hymenomycetes). *Bidr. Till Kännedom Av Finl. Nat. Och Folk.* **1889**, *48*, 1–470.
4. Eriksson, J.; Hjortstam, K.; Ryvarden, L. The Corticiaceae of North Europe volume 5: Mycoaciella–*Phanerochaete*. *Fungiflora Oslo* **1978**, *5*, 987–1047.
5. Burdsall, H.H. A contribution to the taxonomy of the genus *Phanerochaete*. *Mycol. Mem.* **1985**, *10*, 1–165.

6. Wu, S.H. The Corticiaceae (Basidiomycetes) subfamilies Phlebioideae, *Phanerochaetoideae* and Hyphodermoideae in Taiwan. *Acta Bot. Fenn.* **1990**, *142*, 1–123.
7. Wu, S.H. A study of the genus *Phanerochaete* (Aphyllophorales) with brown subicular hyphae. *Mycotaxon* **1995**, *54*, 163–172.
8. Wu, S.-H. Nine new species of *Phanerochaete* from Taiwan. *Mycol. Res.* **1998**, *102*, 1126–1132. [CrossRef]
9. Wu, S.H. Six new species of *Phanerochaete* from Taiwan. *Bot. Bull. Acad. Sin.* **2000**, *41*, 165–174.
10. Wu, S.H. Two new species of *Phanerochaete* from Taiwan. *Mycotaxon* **2004**, *90*, 423–429.
11. Wu, S.H. Three new species of corticioid fungi from Taiwan. *Bot. Stud.* **2007**, *48*, 325–330.
12. Xiong, H.X.; Dai, Y.C. Notes on lignicolous corticioid fungi in China 3. *Phanerochaete* (Basidiomycota, Polyporales) in China. *Mycosystema* **2009**, *28*, 29–35.
13. Wu, S.-H.; Nilsson, H.R.; Chen, C.-T.; Yu, S.-Y.; Hallenberg, N. The white-rotting genus *Phanerochaete* is polyphyletic and distributed throughout the phleboid clade of the Polyporales (Basidiomycota). *Fungal Divers.* **2010**, *42*, 107–118. [CrossRef]
14. Wu, S.-H.; Chen, C.-C.; Wei, C.-L. Three new species of *Phanerochaete* (Polyporales, Basidiomycota). *MycoKeys* **2018**, *41*, 91–106. [CrossRef]
15. Wu, S.-H.; Chen, Y.-P.; Wei, C.-L.; Floudas, D.; Dai, Y.-C. Two new species of *Phanerochaete* (Basidiomycota) and redescription of *P. robusta*. *Mycol. Prog.* **2017**, *17*, 425–435. [CrossRef]
16. Ghobad-Nejhad, M.; Liu, S.-L.; Langer, E.; Dai, Y.-C. Molecular and morphological evidence reveal a new non-cystidiate species belonging to the core *Phanerochaete* (Polyporales). *Mycol. Prog.* **2015**, *14*, 68. [CrossRef]
17. Liu, S.L.; He, S.H. *Phanerochaete* porostereoides, a new species in the core clade with brown generative hyphae from China. *Mycosphere* **2016**, *7*, 648–655. [CrossRef]
18. Chen, C.-C.; Wu, S.-H.; Chen, C.-Y. Hydnophanerochaete and Odontoefibula, two new genera of phanerochaetoid fungi (Polyporales, Basidiomycota) from East Asia. *MycoKeys* **2018**, *39*, 75–96. [CrossRef] [PubMed]
19. Xu, Y.L.; Cao, Y.F.; Nakasone, K.K.; Chen, C.C.; He, S.H. Taxonomy and phylogeny of *Phanerochaete* sensu stricto (Polyporales, Basidiomycota) with emphasis on Chinese collections and descriptions of nine new species. *Mycosphere* **2020**, *11*, 1527–1552. [CrossRef]
20. Binder, M.; Hibbett, D.S.; Larsson, K.; Larsson, E.; Langer, E.; Langer, G. The phylogenetic distribution of resupinate forms across the major clades of mushroom-forming fungi. *Syst. Biodivers.* **2005**, *3*, 113–157. [CrossRef]
21. Floudas, D.; Hibbett, D.S. Revisiting the taxonomy of *Phanerochaete* (Polyporales, Basidiomycota) using a four gene dataset and extensive ITS sampling. *Fungal Biol.* **2015**, *119*, 679–719. [CrossRef]
22. Miettinen, O.; Spirin, V.; Vlasák, J.; Rivoire, B.; Stenroos, S.; Hibbett, D. Polypores and genus concepts in Phanerochaetaceae (Polyporales, Basidiomycota). *MycoKeys* **2016**, *17*, 1–46. [CrossRef]
23. Justo, A.; Miettinen, O.; Floudas, D.; Ortiz-Santana, B.; Sjökvist, E.; Lindner, D.; Nakasone, K.; Niemelä, T.; Larsson, K.-H.; Ryvarden, L.; et al. A revised family-level classification of the Polyporales (Basidiomycota). *Fungal Biol.* **2017**, *121*, 798–824. [CrossRef]
24. Petersen, J.H. The Danish Mycological Society's colour-chart. *Foreningen til Svampekundskabens Fremme Greve* **1996**, *6*, 1–6.
25. Dai, Y.C.; Xiong, H.X. *Flora Fungorum Sinicorum Volume 42 Corticiaceae s.l. (1)*; Science Press: Beijing, China, 2012; 198p.
26. Zhao, C.-L.; Wu, Z.-Q. Ceriporiopsis kunmingensis sp. nov. (Polyporales, Basidiomycota) evidenced by morphological characters and phylogenetic analysis. *Mycol. Prog.* **2016**, *16*, 93–100. [CrossRef]
27. White, T.J.; Bruns, T.; Lee, S.; Taylor, J.W. Amplification and direct sequencing of fungal ribosomal RNA genes for phylogenetics. *PCR Protoc. A Guide Methods Appl.* **1990**, *18*, 315–322.
28. Wang, C.-G.; Vlasák, J.; Dai, Y.-C. Phylogeny and diversity of Bjerkandera (Polyporales, Basidiomycota), including four new species from South America and Asia. *MycoKeys* **2021**, *79*, 149–172. [CrossRef] [PubMed]
29. Zhao, C.; Ren, G.-J.; Wu, F. A new species of Hyphodermella (Polyporales, Basidiomycota) with a poroid hymenophore. *Mycoscience* **2017**, *58*, 452–456. [CrossRef]
30. Telleria, M.T.; Dueñas, M.; Melo, I.; Martín, M.P. Morphological and molecular studies of Hyphodermella in the Western Mediterranean area. *Mycol. Prog.* **2010**, *9*, 585–596. [CrossRef]
31. Vu, D.; Groenewald, M.; De Vries, M.; Gehrmann, T.; Stielow, B.; Eberhardt, U.; Al-Hatmi, A.; Groenewald, J.Z.; Cardinali, G.; Houbraken, J.; et al. Large-scale generation and analysis of filamentous fungal DNA barcodes boosts coverage for kingdom fungi and reveals thresholds for fungal species and higher taxon delimitation. *Stud. Mycol.* **2019**, *92*, 135–154. [CrossRef]
32. Larsson, K.-H. Re-thinking the classification of corticioid fungi. *Mycol. Res.* **2007**, *111*, 1040–1063. [CrossRef]
33. Phookamsak, R.; Hyde, K.D.; Jeewon, R.; Bhat, D.J.; Jones, E.B.G.; Maharachchikumbura, S.; Raspé, O.; Karunarathna, S.C.; Wanasinghe, D.; Hongsanan, S.; et al. Fungal diversity notes 929–1035: Taxonomic and phylogenetic contributions on genera and species of fungi. *Fungal Divers.* **2019**, *95*, 1–273. [CrossRef]
34. Volobuev, S.; Okun, M.; Ordynets, A.; Spirin, V. The *Phanerochaete* sordida group (Polyporales, Basidiomycota) in temperate Eurasia, with a note on *Phanerochaete pallida*. *Mycol. Prog.* **2015**, *14*, 80. [CrossRef]
35. Jia, B.-S.; Zhou, L.-W.; Cui, B.-K.; Rivoire, B.; Dai, Y.-C. Taxonomy and phylogeny of Ceriporia (Polyporales, Basidiomycota) with an emphasis of Chinese collections. *Mycol. Prog.* **2013**, *13*, 81–93. [CrossRef]
36. Sádlíková, M. A new *Phanerochaete* (Polyporales, Basidiomycota) with brown subicular hyphae from Thailand. *Mycosphere* **2017**, *8*, 1024–1030. [CrossRef]

37. Gómez-Montoya, N.; Drechsler-Santos, E.R.; Ferreira-Lopes, V.; Robledo, G.L.; Tomšovský, M.; Urcelay, C. New insights on *Trametopsis* Tomovsk (Polyporales Gum) based on phylogenetic evidences and morphological analyses of neotropical species. *Phytotaxa* **2017**, *311*, 155–167. [CrossRef]
38. Hall, T.A. Bioedit: A user-friendly biological sequence alignment editor and analysis program for Windows 95/98/NT. *Nucleic Acids Symp. Ser.* **1999**, *41*, 95–98.
39. Swofford, D.L. *PAUP: Phylogenetic Analysis Using Parsimony (and Other Methods)*; Version 4.0b10; Sinauer Associates: Sunderland, MA, USA, 2002.
40. Felsenstein, J. Confidence limits on phylogenies: An approach using the bootstrap. *Evolution* **1985**, *39*, 783–791. [CrossRef] [PubMed]
41. Miller, M.A.; Holder, M.T.; Vos, R.; Midford, P.E.; Liebowitz, T.; Chan, L.; Hoover, P.; Warnow, T. The CIPRES Portals. CI-PRES. Available online: http://www.phylo.org/sub_sections/portal (accessed on 9 September 2020).
42. Nylander, J.A.A. MrModeltest v2. Program distributed by the author. Evolutionary Biology Centre, Uppsala University.ampignons de l'Équateur (Pugillus IV). *Bull. L´Herb. Boissier* **2004**, *3*, 53–74.
43. Ronquist, F.; Huelsenbeck, J.P. MrBayes 3: Bayesian phylogenetic inference under mixed models. *Bioinformatics* **2003**, *19*, 1572–1574. [CrossRef]
44. Alshammari, N.; Ameen, F.; AlKahtani, M.; Stephenson, S. Characterizing the assemblage of wood-decay fungi in the forests of northwest Arkansas. *J. Fungi* **2021**, *7*, 309. [CrossRef]
45. Blumenstein, K.; Bußkamp, J.; Langer, G.; Langer, E.; Terhonen, E. The diplodia tip blight pathogen *Sphaeropsis sapinea* is the most common fungus in Scots pines' mycobiome, irrespective of health status—A case study from Germany. *J. Fungi* **2021**, *7*, 607. [CrossRef] [PubMed]
46. Chen, P.Y.; Chuang, Y.C.; Wu, U.I.; Sun, H.Y.; Wang, J.T.; Sheng, W.H.; Chen, Y.C.; Chang, S.C. Mechanisms of azole resistance and trailing in Candida tropicalis bloodstream isolates. *J. Fungi* **2021**, *7*, 612. [CrossRef] [PubMed]
47. Guan, Q.-X.; Zhao, C.-L. Taxonomy and phylogeny of the wood-inhabiting fungal genus *Hyphoderma* with descriptions of three new species from East Asia. *J. Fungi* **2021**, *7*, 308. [CrossRef] [PubMed]
48. Štefániková, J.; Martišová, P.; Šnirc, M.; Kunca, V.; Árvay, J. The effect of *Amanita rubescens* Pers developmental stages on aroma profile. *J. Fungi* **2021**, *7*, 611. [CrossRef]